# Cobalt(III)-Catalyzed Free Amine Directed Site-Selective Allylation in 2-Aminobiaryls with Vinyl Cyclopropanes

Deepan Chowdhury, Suman Ghosh,[†] K.S.S.V. Prasad Reddy,[†] Sharma S.R.K.C. Yamijala and Mahiuddin Baidya*

Department of Chemistry, Indian Institute of Technology Madras, Chennai 600036, India.

ABSTRACT: 2-Aminobiaryls are privileged scaffolds and their cogent synthesis and diversifications, particularly through the C–H bond activation strategy, is a continuous enterprise in organic synthesis. In this realm, capitalization on susceptible native amine (–NH2) directing group is beneficial but increasingly challenging owing to its innate nucleophilic reactivity. Also, the C–H activation reactions of this class of substrates have traditionally been restricted to the cross-ring C–H bond as the *ortho* C–H functionalization presumably requires the formation of a strained high-energy four-membered metallacycle. Herein, we report the first example of free amine-directed *ortho* C–H activation reaction of 2-aminobiaryls under high-valent Cp*Co(III)-catalysis, enabling regio- and stereoselective allylation reaction in high yields. The protocol engages vinyl cyclopropanes as allyl synthons where the C–C bond construction event was tunneled to a C–C activation process to forge internal olefin with exclusive (*E*)-selectivity. The products were judicially used to access high-value benzo[*d*]isoxazoles and dihydro phenanthridine derivatives. Mechanistic experiments and DFT calculations have also been conducted to unravel the rationale behind the unique site selectivity, where the thermodynamic constraints of the corresponding intermediates favoring the *ortho* C–H activation over cross-ring functionalization.
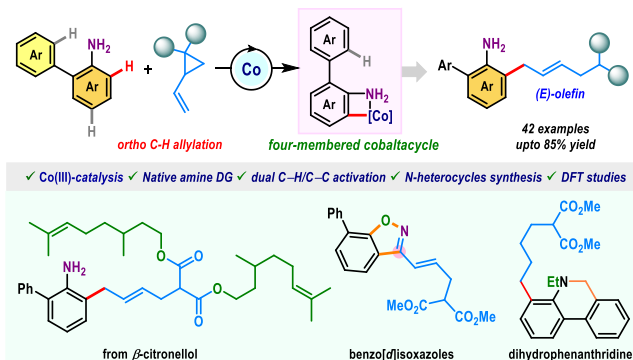
INTRODUCTION

Biaryl scaffolds adorn the core structure of several important natural products, therapeutic agents, and agrochemicals.[1] They also form the backbone of a diverse class of chiral ligands.[1d,e] Consequently, the synthesis and diversification of biaryl molecules have always garnered interest in the synthetic community. While, traditional approaches toward the biaryl scaffolds rely mainly on transition metal-catalyzed cross-coupling reactions[2], in recent years, directed C–H bond activation reactions have come to the fore as they offer step and atom economic disconnections for the synthesis of these molecules.[3] Here, heteroatomic directing groups play an important role by dictating the regioselectivity of these reactions.[4a] In this context, the utilization of common organic functionalities like carboxylic acids, amides, ketones, esters, etc. as directing groups (DGs) is advantageous.[4b,4c] However, unlike the aforementioned functional groups, the potential of the native amine (–NH2) functionality to act as a directing group has not been realized fully (Scheme

1a), despite the ubiquitous distribution of amine or its derivatives in bio-relevant molecules.[5] The dormant progress in this area of research can be attributed to

Scheme 1. Free Amine Directing Group and C–H Bond Activation Reactions of 2-Aminobiaryls
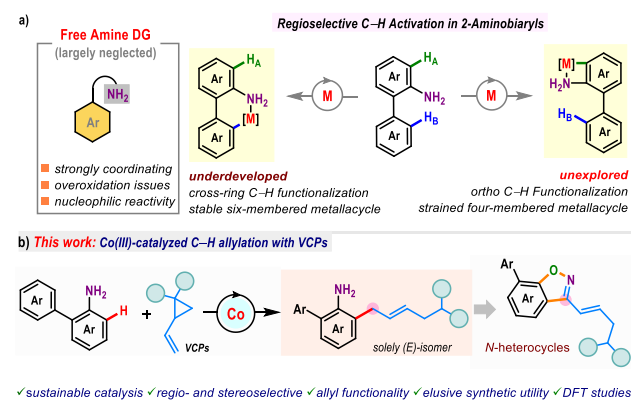
native reactivity of the free amine functionality such as strong coordination with metal catalyst leading to its deactivation, substrate coordination under the reaction conditions, and innate nucleophilic reactivity *en route* to undesired side reactions (Scheme 1a).[6] Thus, exploration of sustainable free amine directed C–H activation reactions is highly desirable. The 2-aminobiaryl motif has been considered as a prototype substrate for free amine directed C–H activation reactions. A closer look into this framework reveals the presence of two alternate sites of directed C–H activation, the *ortho* C–H$_A$ bond and the cross-ring C–H$_B$ bond (Scheme 1a). The functionalization of the cross-ring C–H$_B$ bond requires the formation of a thermodynamically more stable six-membered metallacycle and has been explored to a large extent.[7] In sharp contrast, directed C–H bond activation methodologies that harness the reactivity of the C–H$_A$ bond *ortho* to the free amine unit are highly challenging as such functionalization necessitates the formation of a strained four-membered metallacycle with a high energy barrier (Scheme 1a).[8]
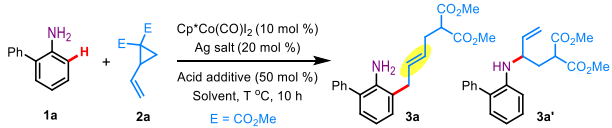
We posited that the adoption of an electrophilic C–H metalation strategy using high-valent Co(III) catalysis could offer an exciting solution.[9] Cobalt being the first-row transition metal with smaller ionic radii would be significantly electrophilic at higher oxidation state[9i-p] and we believe such characteristics would favor the desired metalation in the aniline ring and may be useful to overcome the thermodynamic barrier associated with the formation of strained four-membered cobaltacycle. Of note, this reaction modality is crucial to preserve the *ortho*-selectivity as electrophilic functionalization of anilines often resulted in a mixture of *ortho*- and *para*-functionalized products with poor synthetic utility.[10]

Herein, we demonstrated the first example of such a reaction through the development of a regio- and stereoselective Co(III)-catalyzed C–H allylation of 2-arylanilines with vinyl cyclopropanes (Scheme 1b). While cobalt encompasses a relatively nontoxic portfolio with a high abundance in the earth's crust, favoring sustainable catalysis, the products of this process are functionally enriched with amine and allyl motifs which were engaged to prepare valuable benzo[*d*]isoxazole and dihydrophenanthridine frameworks. DFT studies were also performed to support the reaction mechanism. In this work, the critical challenge is grounded in the synchronous control of regioselective C–H bond activation through a strained metalacycle, regioselective opening of vinyl cyclopropane[11] that involves a C–C bond activation, and the stereochemistry of the internal olefin bestowed in the allylation product.

RESULTS AND DISCUSSION

We commenced investigations following the model reaction between 2-phenylaniline **1a** and vinylcyclopropane **2a** (Table 1). Our initial attempts turned out challenging as the exposure of **1a** and **2a** to Cp*Co(CO)I$_2$ catalyst in presence of 1-AdCOOH as additive and AgSbF$_6$ as halide
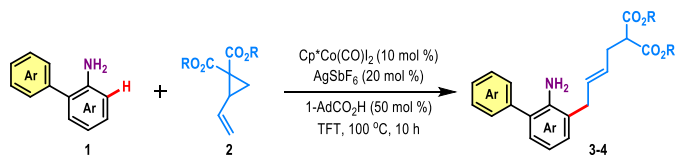
Table 1. Reaction Optimization[*a*]

entry	solvent	acid additive	Ag salt	T (°C)	yield (%)[*b*]	
					3a	**3a'**
1	THF	1-AdCO$_2$H	AgSbF$_6$	80	–	59
2	DCE	1-AdCO$_2$H	AgSbF$_6$	80	–	65
3	TFE	1-AdCO$_2$H	AgSbF$_6$	80	32	55
4	HFIP	1-AdCO$_2$H	AgSbF$_6$	80	34	51
5	TFT	1-AdCO$_2$H	AgSbF$_6$	80	63	18
6	Toluene	1-AdCO$_2$H	AgSbF$_6$	80	54	26
7	TFT	MesCO$_2$H	AgSbF$_6$	80	41	22
8	**TFT**	**1-AdCO$_2$H**	**AgSbF$_6$**	**100**	**78**	**< 5**
9[*c*]	TFT	1-AdCO$_2$H	–	100	65	18
10	TFT	1-AdCO$_2$H	AgNTf$_2$	100	53	< 5
11	TFT	–	AgSbF$_6$	100	–	trace
12	TFT	1-AdCO$_2$H	–	100	–	trace

[*a*]Reaction conditions: **1a** (0.3 mmol), **2a** (0.33 mmol), solvent (3.0 mL) for 10 h under argon atmosphere. [*b*]Isolated yields were provided.
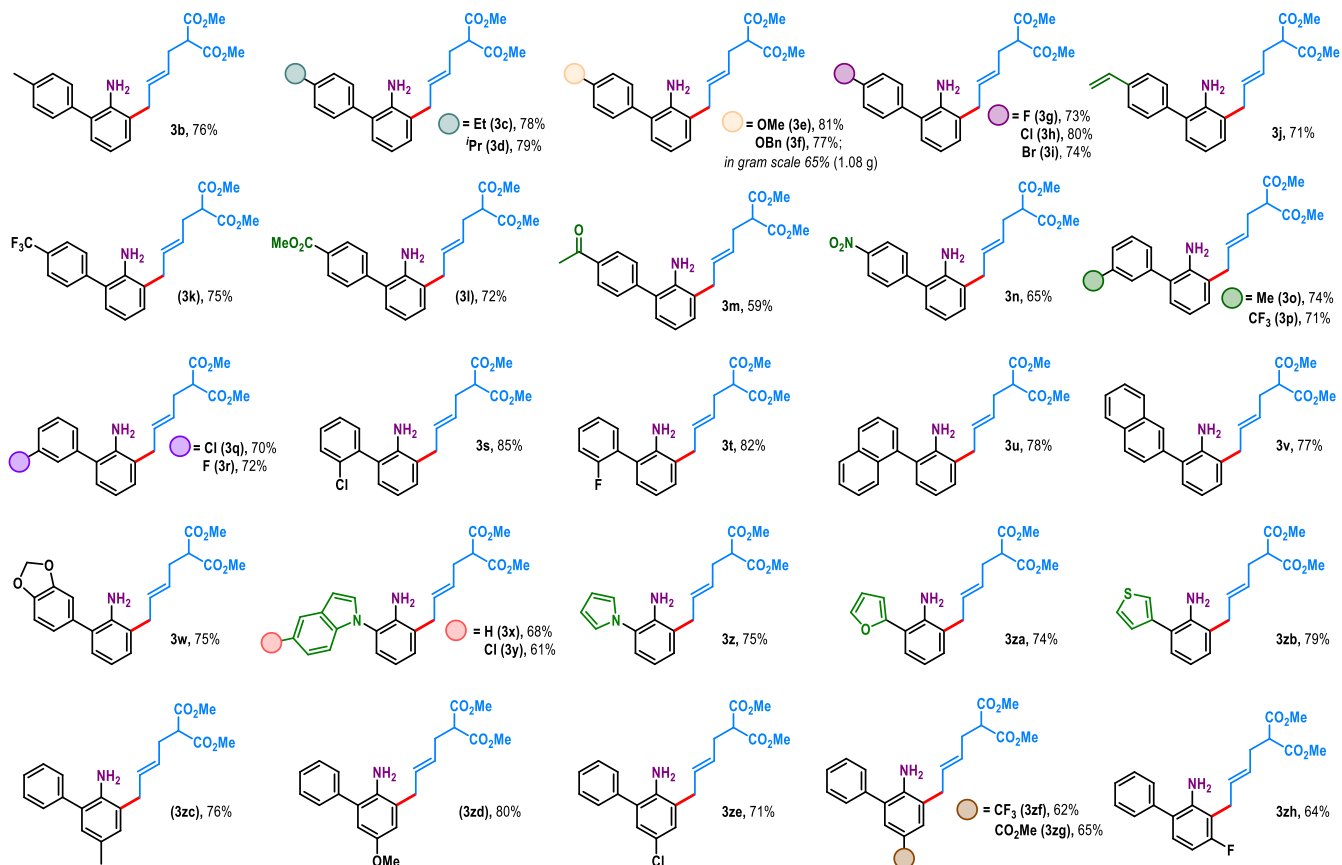
ion scavenger in THF or DCE solvent at 80 °C gave only undesired *N*-adduct **3a'** (entries 1-2). We first noticed the formation of the desired C–H bond activation product **3a** when the reaction was conducted in CF$_3$CH$_2$OH (TFE), albeit in a poor yield of 32% (entry 3). Further alteration o reaction solvent to HFIP did not improve the situation and the *N*-attack product was still formed in major amounts (entry 4). However, in trifluorotoluene (TFT) solvent, product selectivity was reversed, favoring the desired C–H activation product with 63% isolated yield (entry 5). The selectivity was also unchanged in toluene solvent; however, the reaction efficacy was moderate (entry 6). The replacement of 1-AdCO$_2$H with MesCO$_2$H reduced the yield of **3a** considerably (entry 7). Satisfyingly, when the reaction temperature was increased to 100 °C, yield and selectivity both improved significantly, offering *ortho*-functionalized product **3a** in 78% yield (entry 8). At this juncture, the undesired product from *N*-adduct was formed in a negligible amount (< 5% yield). Also, the olefin geometry was exclusively *trans* and no *para*-functionalization product was formed. The use of [Cp*Co(MeCN)$_3$][SbF$_6$]$_2$ as a catalyst was also effective for this reaction, although the desired product was isolated in reduced yield (entry 9). Consideration of AgNTf$_2$ additive provided detrimental outcomes (entry 10). The presence of both additives, acid as well as silver salt, was critical and the reaction was unproductive in the absence of any of them (entries 11-12).

Having finalized the optimal conditions (entry 8, Table 1), the scope of the C–H allylation protocol was explored (Scheme 2). The reaction is quite general for a wide range
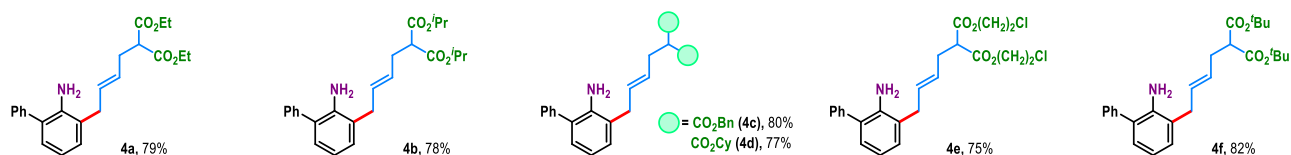
Scheme 2. Substrate Scope in Co(III)-Catalyzed C–H Allylation of 2-Aminobiaryls
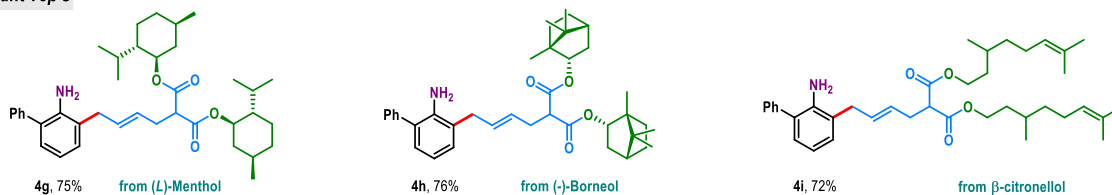
Reaction conditions: **1** (0.3 mmol), **2** (0.33 mmol), TFT (3.0 mL) for 10 h under argon atmosphere. Isolated yields were provided.

of substrates. 2-Aminobiaryls encompassing electron-donating substituents like alkyl (**3b–d**) and alkoxy (**3e–f**) produced desired products in high yields. The reaction was amenable to halogen (**3g-i**) and sensitive vinyl (**3j**) substituents. Electron-withdrawing substituents like trifluoromethyl (**3k**), ester (**3l**), keto (**3m**), and nitro (**3n**)

were also well tolerated. Biaryls bearing *meta-* and *ortho-* substituents in the aryl ring were also suitable to furnish **3o–3t** in high yields. The presence of bulky 1-naphthyl, 2-naphthyl, and 1,3-benzodioxolyl motifs did not hamper the reaction, giving **3u–3w** in 75-78% yields. Substrates with heterocyclic frameworks such as indole (**3x–3y**), pyrrole (**3z**), furan (**3za**), and thiophene (**3zb**) also exhibited smooth reactivity to dispense desired products in good yields. The scope of the reaction was also evaluated with 2-phenylanilines containing common functional groups in *para-* and *meta-*positions of the aniline ring. Methyl (**3zc**), methoxy (**3zd**), and chloride (**3ze**) functionalities rendered high yields (71%–80%), while trifluoromethyl (**3zf**), ester (**3zg**), and fluoro (**3zh**) groups offered slightly reduced yields (62%–65%). Intriguingly, in all cases, products were isolated with excellent regio (*ortho*) and stereoselectivity (*E*-olefin).

Next, the variation in vinylcyclopropanes (VCPs) was examined where 1,1-diester unit prepared from primary (**4a**, **4c**), secondary (**4b**, **4d**) as well as tertiary (**4f**) alcohols, effortlessly delivered allylation products in uniformly high yields (Scheme 2). The VCP obtained from 2-chloroethanol offered desired product **4e** in 75% yield. The reactivity of VCPs derived from biomolecules like menthol (**4g**), borneol (**4h**), and β-citronellol (**4i**) was also investigated. Delightfully, they were equally effective to furnish the C–H allylated 2-phenylanilines in very high yields with exclusive *E*-selectivity (Scheme 2).

Scheme 3. Synthesis of Benzo[*d*]isoxazoles via Oxidation of C–H allylation Products
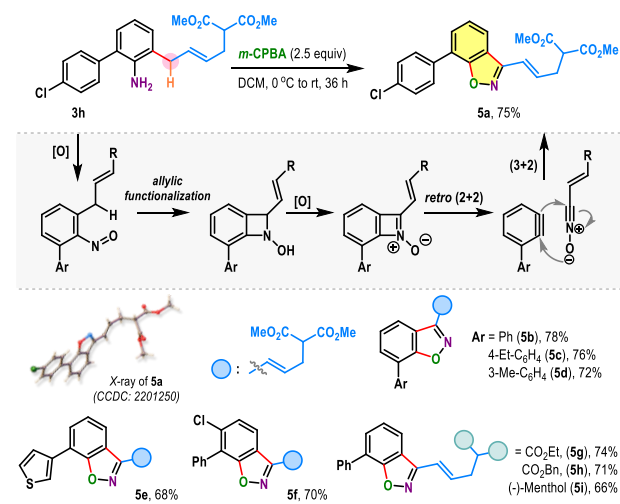

To adorn the synthetic utility, several post-synthetic modifications were performed. We considered nitroso-functionality-based allylic C–H functionalization by converting free amine into a nitroso group (Scheme 3). Accordingly, product **3h** was treated with *m*-CPBA oxidant in DCM solvent at room temperature, which produced functionalized benzo[*d*]isoxazole **5a** in 75% yield. The formation of **5a** can be rationalized through [3+2] cy-

cloaddition reaction of in situ generated nitrone intermediate as depicted in Scheme 3. The structure of benzo[*d*]isoxazole product **5a** was also confirmed through single-crystal *X*-ray analysis. Notably, while the allyl C–H bond in **3h** promotes this unique transformation, the oxidation conditions did not affect the olefin functionality. The protocol can be extended to other C–H allyllated products to furnish **5b–5i** in good yields (Scheme 3).
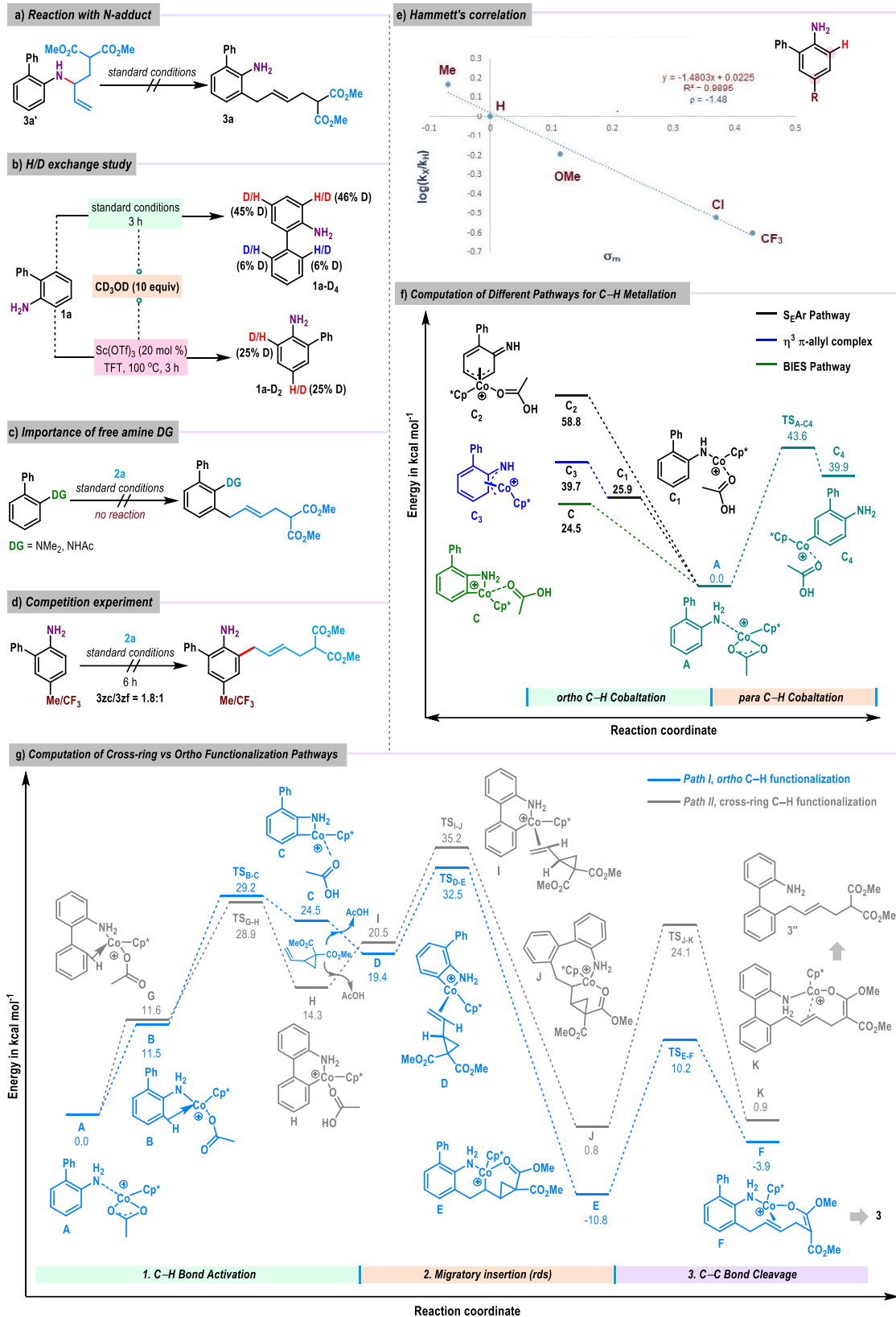
The Pd/C mediated hydrogenation of product **3a** was also executed. In this case, along with hydrogenation of the double bond, *N*-alkylation of amine functionality took place to give **6a** in 85% yield (Scheme 4a). The formation of **6a** can be attributed to the transfer hydrogenation-based reductive amination process.[12] Subsequently, **6a** was subjected to aza-Mannich cyclization in the presence of paraformaldehyde and a catalytic amount of *p*-TsOH.H$_2$O to access dihydrophenanthridine derivative **7a** in 92% yield (Scheme 4a). Through LiAlH$_4$ reduction 1,3-diols **8a** and **8b** were prepared in high yields (Scheme 4b). Further, the Krapcho decarboxylation process was also performed to prepare monoester **9a** and **9b** in 76% and 79% yields, respectively (Scheme 4c).

Scheme 4. Post-functionalization of C–H Allylation Products
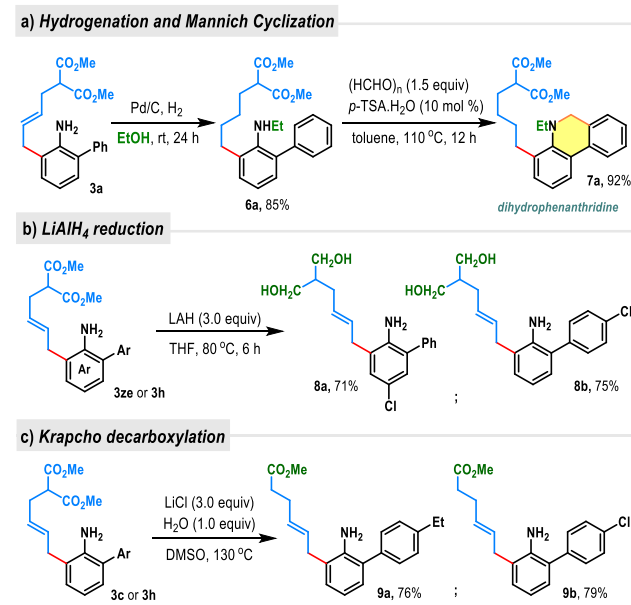
To delineate the mode of action of this Co(III)-catalyzed process, we conducted various mechanistic studies. Whether the reaction proceeds via an initial nucleophilic attack of the amine functionality on VCP followed by thermal/Lewis acid mediated Hofmann-Martius type rearrangement giving rise to the *ortho* allylated product was an intriguing question. To address this issue, the isolated *N*-adduct **3a'** was treated under the standard reaction conditions. However, no rearrangement of **3a'** to **3a** was detected, refuting the intermediacy of **3a'** in

**Scheme 5. Mechanistic Studies and DFT Calculation (wB97XD/6-31+G(d,p)-LanL2DZ-PCM(1,2-Dichloroethane)**

a) Reaction with N-adduct

MeO$_2$C   CO$_2$Me

Ph / N / H — 3a'

standard conditions ⫽→

Ph / NH$_2$ / CO$_2$Me / CO$_2$Me — 3a

b) H/D exchange study

Ph / H$_2$N — 1a

standard conditions 3 h →

D/H (45% D)   H/D (46% D)   NH$_2$ D/H (6% D)   H/D (6% D)   1a-D$_4$

CD$_3$OD (10 equiv)

Sc(OTf)$_3$ (20 mol %) TFT, 100 °C, 3 h →

D/H (25% D)   NH$_2$ Ph   H/D (25% D)   1a-D$_2$

c) Importance of free amine DG

Ph / DG

standard conditions 2a no reaction ⫽→

Ph / DG / CO$_2$Me / CO$_2$Me

DG = NMe$_2$, NHAc

d) Competition experiment

Ph / NH$_2$ / Me/CF$_3$

2a standard conditions 6 h ⫽ 3zc/3zf = 1.8:1 →

Ph / NH$_2$ / CO$_2$Me / CO$_2$Me / Me/CF$_3$

e) Hammett's correlation

y = -1.4803x + 0.0225
R² = 0.9895
ρ = -1.48

log(k$_X$/k$_H$) vs σ$_m$

Me, H, OMe, Cl, CF$_3$

Ph / NH$_2$ / H / R

f) Computation of Different Pathways for C−H Metallation

— S$_E$Ar Pathway
— η^3 π-allyl complex
— BIES Pathway

Energy in kcal mol^{-1}

C$_2$ 58.8
C$_3$ 39.7
C$_1$ 25.9
C 24.5
A 0.0
TS$_{A-C4}$ 43.6
C$_4$ 39.9

ortho C−H Cobaltation   para C−H Cobaltation

Reaction coordinate

g) Computation of Cross-ring vs Ortho Functionalization Pathways

Path I, ortho C−H functionalization
Path II, cross-ring C−H functionalization

Energy in kcal mol^{-1}

A 0.0
B 11.5
G 11.6
TS$_{B-C}$ 29.2
TS$_{G-H}$ 28.9
C 24.5
H 14.3
I 20.5
D 19.4
TS$_{I-J}$ 35.2
TS$_{D-E}$ 32.5
J 0.8
E -10.8
TS$_{J-K}$ 24.1
TS$_{E-F}$ 10.2
K 0.9
F -3.9

3''
3

1. C−H Bond Activation   2. Migratory insertion (rds)   3. C−C Bond Cleavage

Reaction coordinate

this process (Scheme 5a). Next, we treated 2-aminobiphenyl **1a** with excess CD$_3$OD under the standard catalytic conditions where we found a considerable amount of deuterium incorporation in the aniline ring and slight H/D-exchange in the cross-ring C–H bonds (Scheme 5b). This observation suggested the operation of a reversible C–H cobaltation process. Notably, deuterium incorporation also occurred at the *para*-position of the aniline ring; however, we never detected the *para*-functionalized product during our investigation. Of note, we observed around 25% deuterium incorporation in the aniline ring when Sc(OTf)$_3$ Lewis acid was employed instead of Co(III)-catalyst (Scheme 5b). Thus, deuterium incorporation via Friedel Crafts type electrophilic aromatic substitution reaction cannot be ignored; however, the contribution of this process is lower for the overall C–H/C–D exchange event. Also, free amine functionality is critical for this reaction as protected *N,N*-dimethyl or *N*-acetyl substrate was unable to promote this reaction (Scheme 5c). These findings signify the indispensable role of the free amine motif as a directing group that favors the *ortho*-functionalized product. A competition experiment between electronically different substrates revealed that the reaction with electron-rich methyl-substituted aniline proceeds 1.8 times faster compared to the electron-deficient trifluoromethyl derivative (Scheme 5d). Further, for this reaction, we found the Hammett correlation with a negative ρ value ($\rho = -1.48$), implying the decrease of electron density in the aniline ring during the C–H activation step and the development of a positive charge in the transition state (Scheme 5e). Findings from both of these studies collectively satisfy the requirements of C–H scission protocol likely operating via a base-assisted internal electrophilic substitution (BIES) mechanism.[13]

To gain additional mechanistic insights, we performed DFT calculations (Scheme 5f-g).[14] At the onset, we computed the energies associated with probable *ortho*-metallated species arising from cobalt complex **A** (Scheme 5g). Our control experiments suggested a BIES type C–H activation process which will generate the four-membered cobaltacycle **C** and we obtained 24.5 kcal/mol energy for this cobalt complex. The desired metalation event can also occur via initial N–H deprotonation followed by classical electrophilic aromatic substitution reaction, which garners the dearomatized Wheland intermediate. The initial deprotonation will give the cobalt complex **C$_1$** having anionic coordination to amine. Its energy was 25.9 kcal/mol higher than the cobalt complex **A** having neutral coordination between the amine and cobalt catalyst. The energy of the metallated species **C$_2$** arising from A via S$_E$Ar mechanism and harnessing a η^3 π-allyl coordination with cobalt turned out 58.8 kcal mol^{-1}. The complex **C$_1$** can also transform into the η^3 π-allyl cobalt complex **C$_3$**, which was found to have an energy of 39.7 kcal/mol. We also calculated the energy of the cobalt complex **C$_4$** forming via *para*-C–H bond activation; however, it was considerably high (39.9 kcal mol^{-1}). Overall, the cobalt complex **C** with significantly lower energy is most suitable and was considered to com-

pute the full mechanistic profile of this reaction. A comparison with the cross-ring functionalization was also considered to unravel the unique site selectivity. In Scheme 5h, *Path I* (denoted by blue line) depicts the formation of the *ortho*-functionalized product **3** and *Path II* (denoted by grey line) accounts for the formation of cross-ring functionalized product **3′′**. The reaction commences with the free amine-directed, carboxylate-assisted C–H activation leading to the formation of respective cobaltacycles. We found that the barrier for the formation of the cobaltacyle **C** via transition state **TS$_{B-C}$** was about 29.2 kcal mol^{-1}, which was comparable to the cobaltacycle **H** (28.9 kcal mol^{-1}) formed via transition state **TS$_{G-H}$**. The next step involves ligand exchange with vinyl cyclopropane generating intermediate **D** (19.4 kcal mol^{-1}) and intermediate **I** (20.5 kcal mol^{-1}) for *Path I* and *Path II* respectively. Notably, this step is exergonic for *Path I* by 5.1 kcal/mol. The subsequent migratory insertion of the vinyl cyclopropane into the cobaltacycle was found to be the rate-determining step of the reaction. The energy barrier for the **TS$_{D-E}$** to give intermediate **E** was about 2.7 kcal mol^{-1} lower when compared with **TS$_{I-J}$** leading to the intermediate **J**. In addition, this insertion step was highly exergonic with the release of 30.2 kcal/mol energy for *Path I*. Further, our calculation revealed that the C–C bond cleavage event was also favorable for *path I* with an activation barrier of 21.0 kcal/mol as compared to 24.1 kcal/mol for *path II*. Also, the intermediate **F** (-3.9 kcal mol^{-1}) resulting from C–C bond cleavage step in *path I* is much more stable than the intermediate **L** (0.9 kcal mol^{-1}) in *path II*. Overall, these results indicate that *path I* is energetically favorable. Most likely, lower free energy barriers associated with **TS$_{D-E}$** and **TS$_{E-F}$** as well as the higher stability of intermediates **E** and **F** govern the *ortho* selectivity for this process.

Scheme 6. Plausible Mechanism
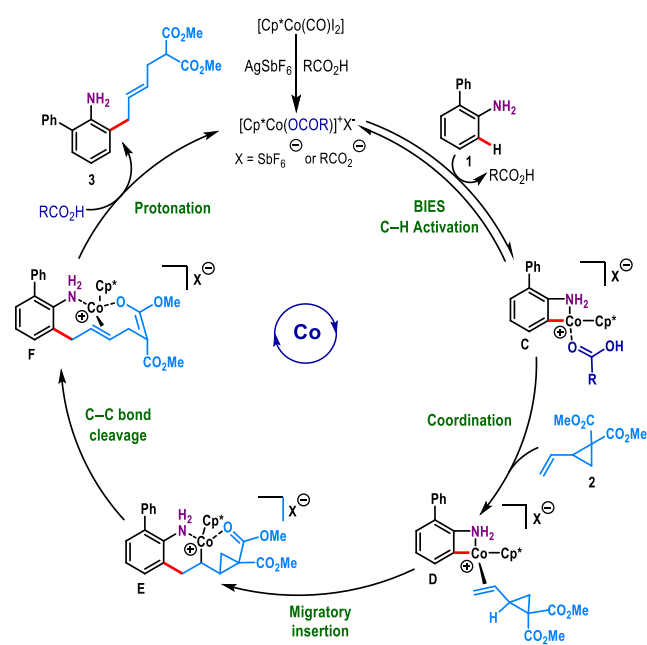
Based on the mechanistic experiments and theoretical calculations, a general catalytic cycle for the protocol is

presented in Scheme 6. Initially, the catalytically competent cationic Co(III) species is generated from the precursor [Cp*Co(CO)I$_2$] and engages in a regioselective C–H cleavage of 2-aminobiaryl substrate **1**. This step is reversible in nature and operates via a BIES mechanism leading to the four-membered cobaltacycle **C**. Ligand exchange, coordination, and subsequent migratory insertion of vinyl cyclopropane then lead to the formation of intermediate **E**. Next, this intermediate undergoes C–C bond cleavage to give intermediate **F**. The geometry of the olefin is dictated by this step. Finally, protodemetalation liberates the allylation product **3** with the regeneration of the active Co(III) catalyst to continue the cycle.

In conclusion, we have developed for the first time a Cp*Co(III)-catalyzed site-selective C–H activation/C–C bond formation cascade reaction in 2-aminobiaryls using vinyl cyclopropanes as synthons. The reaction features regioselective insertion/cyclopropane ring opening event and offers *ortho*-allylation products in high yields. The reaction scope was broad encompassing both electron-donating and withdrawing functionalities and olefins were obtained with exclusive *E*-selectivity. The synthetic potential of this strategy was highlighted through product diversification, which gives facile access to valuable heterocycles such as benzo[*d*]isoxazoles and phenanthridine derivatives. The rationale behind the unique site selectivity was unraveled using both experimental and theoretical methods. The thermodynamic stability of the observed product drives the reaction in its desired pathway, overcoming the kinetic barrier associated with the formation of a strained cobaltacycle.

ASSOCIATED CONTENT

Supporting Information
Complete experimental details, characterization data for the prepared compounds, Cartesian coordinates of DFT optimized structures, and crystallographic data are available in the supporting information.

AUTHOR INFORMATION

Corresponding Author
Prof. Mahiuddin Baidya, Department of Chemistry, Indian Institute of Technology, Madras, Chennai-600036, India. Email: mbaidya@iitm.ac.in

Author Contributions
The manuscript was written through the contributions of all authors. All authors have given approval for the final version of the manuscript. †These authors contributed equally to this work.

REFERENCES
1. (a) Zask, A.; Murphy, J.; Ellestad, G. A. Biological Stereoselectivity of Atropisomeric Natural Products and Drugs. *Chirality* **2013**, *25*, 265-274. (b) Wang, Y.; Cai, W.; Cheng, Y.; Yang, T.; Liu, Q.; Zhang, G.; Meng, Q.; Han, F.; Huang, Y.; Zhou, L.; Xiang, Z.; Zhao, Y-G.; Xu, Y.; Cheng, Z.; Lu, S.; Wu, Q.; Xiang, J-N.; Eliott, J.D.; Leung, S.; Ren, F.; Lin, X. Discovery of Biaryl Amides as Potent, Orally Bioavailable, and CNS Penetrant ROR γ t Inhibitors. *ACS. Med. Chem. Lett.* **2015**, *6*, 787-792. (c) Chen, T.; Xiong, H.; Yang, J. F.; Zhu, X. L.; Qu, R. Y.; Yang, G. F. Diaryl Ether: A Privileged Scaffold for Drug and Agrochemical Discovery. *J. Agric. Food Chem.* **2020**, *68*, 9839-9877. (d) Surry, D. S.; Buchwald, S. L. Biaryl Phosphane Ligands in Palladium-Catalyzed Amination. *Angew. Chem., Int. Ed.* **2008**, *47*, 6338-6361. (e) Yue, Q.; Liu, B.; Liao, G.; Shi, B. F. Binaphthyl Scaffold: A Class of Versatile Structure in Asymmetric C–H Functionalization. *ACS Catal.* **2022**, *12*, 9359-9396.

2. (a) Kozlowski, M. C.; Morgan, B. J.; Linton, E. C. Total Synthesis of Chiral Biaryl Natural Products by Asymmetric Biaryl Coupling. *Chem. Soc. Rev.* **2009**, *38*, 3193-3207. (b) García-López, J. A.; Greaney, M. F. Synthesis of Biaryls Using Aryne Intermediates. *Chem. Soc. Rev.* **2016**, *45*, 6766–6798. (c) Piontek, A.; Bisz, E.; Szostak, M. Iron-Catalyzed Cross-Couplings in the Synthesis of Pharmaceuticals: In Pursuit of Sustainability. *Angew. Chem., Int. Ed.* **2018**, *57*, 11116–11128. (d) Zhang, Y. F.; Shi, Z. J. Upgrading Cross-Coupling Reactions for Biaryl Syntheses. *Acc. Chem. Res.* **2019**, *52*, 161-169.

3. (a) Yuan, S.; Chang, J.; Yu, B. Construction of Biologically Important Biaryl Scaffolds through Direct C–H Bond Activation: Advances and Prospects; Springer International Publishing, **2020**; Vol. 378. For selected reviews on Directed C–H Activation reactions, see: (b) Ackermann, L. Carboxylate-Assisted Transition-Metal-Catalyzed C–H Bond Functionalizations: Mechanism and Scope. *Chem. Rev.* **2011**, *111*, 1315-1345. (c) Wencel-Delord, J.; Dröge, T.; Liu, F.; Glorius, F. Towards Mild Metal-Catalyzed C–H Bond Activation. *Chem. Soc. Rev.* **2011**, *40*, 4740–4761. (d) Engle, K. M.; Mei, T.; Wasa, M.; Yu, J. Weak Coordination as a Powerful Means for Developing Broadly Useful C–H Functionalization Reactions. *Acc. Chem. Res.* **2012**, *45*, 788–802. (e) Daugulis, O.; Roane, J.; Tran, L. D. Bidentate, Monoanionic Auxiliary-Directed Functionalization of Carbon-Hydrogen Bonds. *Acc. Chem. Res.* **2015**, *48*, 1053–1064. (f) Hartwig, J. F. Evolution of C–H Bond Functionalization from Methane to Methodology. *J. Am. Chem. Soc.* **2016**, *138*, 2–24. (g) Park, Y.; Kim, Y.; Chang, S. Transition Metal-Catalyzed C–H Amination: Scope, Mechanism, and Applications. *Chem. Rev.* **2017**, *117*, 9247–9301. (h) He, J.; Wasa, M.; Chan, K. S. L.; Shao, Q.; Yu, J. Q. Palladium-Catalyzed Transformations of Alkyl C–H Bonds. *Chem. Rev.* **2017**, *117*, 8754–8786. (i) Wang, C. S.; Dixneuf, P. H.; Soulé, J. F. Photoredox Catalysis for Building C–C Bonds from C(sp^2)–H Bonds. *Chem. Rev.* **2018**, *118*, 7532–7585. (j) Ackermann, L. Metalla-Electrocatalyzed C–H Activation by Earth-Abundant 3d Metals and Beyond. *Acc. Chem. Res.* **2020**, *53*, 84–104. (k) Dalton, T.; Faber, T.; Glorius, F. C–H Activation: Toward Sustainability and Applications. *ACS Cent. Sci.* **2021**, *7*, 245–261.

4. (a) De Sarkar, S.; Liu, W.; Kozhushkov, S. I.; Ackermann, L. Weakly Coordinating Directing Groups for Ruthenium(II)–Catalyzed C–H Activation. *Adv. Synth. Catal.* **2014**, *356*, 1461-1479. (b) Murali, K.; Machado, L. A.; Carvalho, R. L.; Pedrosa, L. F.; Mukherjee, R.; Da Silva Júnior, E. N.; Maiti, D. Decoding Directing Groups and Their Pivotal Role in C–H Activation. *Chem. -*

A Eur. J. **2021**, *27*, 12453-12508. (c) Mandal, R.; Garai, B.; Sundara-raju, B. Weak-Coordination in C–H Bond Functionalizations Catalyzed by 3d Metals. *ACS Catal.* **2022**, *12*, 3452-3506.

5. (a) Hili, R.; Yudin, A. K. Making Carbon-Nitrogen Bonds in Biological and Chemical Synthesis. *Nat. Chem. Biol.* **2006**, *2*, 284-287. (b) McGrath, N. A.; Brichacek, M.; Njardarson, J. T. A Graphical Journey of Innovative Organic Architectures That Have Improved Our Lives. *J. Chem. Educ.* **2010**, *87*, 1348-1349. (c) Roughley, S. D.; Jordan, A. M. The Medicinal Chemist's Toolbox: An Analysis of Reactions Used in the Pursuit of Drug Candidates. *J. Med. Chem.* **2011**, *54*, 3451-3479.

6. He, C.; Whitehurst, W. G.; Gaunt, M. J. Palladium-Catalyzed C(sp³)–H Bond Functionalization of Aliphatic Amines. *Chem* **2019**, *5*, 1031-1058. (b) Ghosh, P.; Chowdhury, D.; Dana, S.; Baidya, M. Transition Metal Catalyzed Free-Amine (–NH₂) Directed C–H Bond Activation and Functionalization for Biaryl Frameworks. *Chem. Rec.* **2021**, *21*, 3795-3817.

7. For selected reports on free amine directed C–H activation using six-membered metallacycles, see: (a) Liang, Z.; Ju, L.; Xie, Y.; Huang, L.; Zhang, Y. Free-Amine-Directed Alkenylation of C(sp²)–H and Cycloamination by Palladium Catalysis. *Chem. - A Eur. J.* **2012**, *18*, 15816-15821. (b) Suzuki, C.; Hirano, K.; Satoh, T.; Miura, M. Ruthenium-Catalyzed Regioselective C–H Alkenylation Directed by a Free Amino Group. *Org. Lett.* **2013**, *15*, 3990-3993. (c) Zuo, Z.; Liu, J.; Nan, J.; Fan, L.; Sun, W.; Wang, Y.; Luan, X. Highly Stereoselective Synthesis of Imine-Containing Dibenzo[*b,d*]Azepines by a Palladium(II)-Catalyzed [5+2] Oxidative Annulation of *o*-Arylanilines with Alkynes. *Angew. Chem., Int. Ed.* **2015**, *54*, 15385-15389. (d) Suzuki, C.; Hirano, K.; Satoh, T.; Miura, M. Direct Synthesis of N–H Carbazoles via Iridium(III)-Catalyzed Intramolecular C–H Amination. *Org. Lett.* **2015**, *17*, 1597–1600. (e) Bai, P.; Huang, X. F.; Xu, G. D.; Huang, Z. Z. Cascade C–H Functionalization/Amidation Reaction for Synthesis of Azepinone Derivatives. *Org. Lett.* **2016**, *18*, 3058-3061. (f) Chowdhury, D.; Dana, S.; Mandal, A.; Baidya, M. A Ruthenium-Catalyzed Free Amine Directed (5+1) Annulation of Anilines with Olefins: Diverse Synthesis of Phenanthridine Derivatives. *Chem. Commun.* **2019**, *55*, 11908-11911. (g) Chowdhury, D.; Dana, S.; Maity, S.; Baidya, M. Ruthenium-Catalyzed Site- Selective C–H Bond Activation/Annulation Cascade toward Dibenzoazepinone Skeletons. *Org. Lett.* **2020**, *22*, 6760-6764. (h) V, D.; Singam, M. K. R.; Vavilapalli, S.; Nanubolu, J. B.; Sridhar Reddy, M. Propargyl Alcohols as Bifunctional Reagents for Divergent Annulations of Biphenylamines via Dual C–H Functionalization/Dual Oxidative Cyclization. *Angew. Chem., Int. Ed.* **2022**, DOI: 10.1002/anie.202215825.

8. (a) McNally, A.; Haffemayer, B.; Collins, B. S. L.; Gaunt, M. J. Palladium-Catalysed C–H Activation of Aliphatic Amines to Give Strained Nitrogen Heterocycles. *Nature* **2014**, *510*, 129-133. (b) He, C.; Gaunt, M. J. Ligand-Enabled Catalytic C–H Arylation of Aliphatic Amines by a Four-Membered-Ring Cyclopalladation Pathway. *Angew. Chem., Int. Ed.* **2015**, *54*, 15840-15844. (c) Meng, K.; Li, T.; Yu, C.; Shen, C.; Zhang, J.; Zhong, G. Geminal Group-Directed Olefinic C–H Functionalization via Four- to Eight-Membered Exo-Metallocycles. *Nat. Commun.* **2019**, *10*, 5109. (d) Wen, J.; Wang, D.; Qian, J.; Wang, D.; Zhu, C.; Zhao, Y.; Shi, Z. Rhodium-Catalyzed P(III)-Directed *ortho*-C–H Borylation of Arylphosphines. *Angew. Chem., Int. Ed.* **2019**, *58*, 2078-2082. (e) Su, B.; Bunescu, A.; Qiu, Y.; Zuend, S. J.; Ernst, M.; Hartwig, J. F. Palladium-Catalyzed Oxidation of β-C(Sp³)–H Bonds of Primary Alkylamines through a Rare Four-Membered Palladacycle Intermediate. *J. Am. Chem. Soc.* **2020**, *142*, 7912-7919. (f) Li, X.; Shen, Y.; Zhang, G.; Zheng, X.; Zhao, Q.; Song, Z. Ru(II)-Catalyzed Decarbonylative Alkylation and Annulations of Benzaldehydes with Iodonium Ylides under Chelation Assistance. *Org. Lett.* **2021**, *24*, 5281-5286.

9. For selected reviews on high-valent Co(III)-catalyzed C–H activation reactions, see: (a) Gandeepan, P.; Cheng, C. H. Cobalt Catalysis Involving π Components in Organic Synthesis. *Acc. Chem. Res.* **2015**, *48*, 1194–1206. (b) Yoshikai, N. Cp*CoIII-Catalyzed C–H Activation of (Hetero) Arenes: Expanding the Scope of Base-Metal-Catalyzed C–H Functionalizations. *ChemCatChem.* **2015**, *7*, 732–734. (c) Moselage, M.; Li, J.; Ackermann, L. Cobalt-Catalyzed C–H Activation. *ACS Catal.* **2016**, *6*, 498–525. (d) Wei, D.; Zhu, X.; Niu, J. L.; Song, M. P. High-Valent-Cobalt-Catalyzed C–H Functionalization Based on Concerted Metalation-Deprotonation and Single-Electron-Transfer Mechanisms. *ChemCatChem.* **2016**, *8*, 1242–1263. (e) Yoshino, T.; Matsunaga, S. (Pentamethylcyclopentadienyl)Cobalt(III)-Catalyzed C–H Bond Functionalization: From Discovery to Unique Reactivity and Selectivity. *Adv. Synth. Catal.* **2017**, *359*, 1245–1262. (f) Baccalini, A.; Vergura, S.; Dolui, P.; Zanoni, G.; Maiti, D. Recent Advances in Cobalt-Catalysed C–H Functionalizations. *Org. Biomol. Chem.* **2019**, *17*, 10119–10141. (g) Han, J. F.; Guo, P.; Zhang, X. G.; Liao, J. Bin; Ye, K. Y. Recent Advances in Cobalt-Catalyzed Allylic Functionalization. *Org. Biomol. Chem.* **2020**, *18*, 7740–7750. (h) Lukasevics, L.; Cizikovs, A.; Grigorjeva, L. C–H Bond Functionalization by High-Valent Cobalt Catalysis: Current Progress, Challenges and Future Perspectives. *Chem. Commun.* **2021**, *57*, 10827-10841. For selected pioneering reports on high-valent Co(III)-catalyzed C–H activation reactions, see: (i) Yoshino, T.; Ikemoto, H.; Matsunaga, S.; Kanai, M. A Cationic High-Valent Cp*Co(III) Complex for the Catalytic Generation of Nucleophilic Organometallic Species: Directed C–H Bond Activation. *Angew. Chem., Int. Ed.* **2013**, *52*, 2207-2211. (j) Yu, D. G.; Gensch, T.; De Azambuja, F.; Vásquez-Céspedes, S.; Glorius, F. Co(III)-Catalyzed C–H Activation/Formal SN-Type Reactions: Selective and Efficient Cyanation, Halogenation, and Allylation. *J. Am. Chem. Soc.* **2014**, *136*, 17722-17725. (k) Nakanowatari, S.; Mei, R.; Feldt, M.; Ackermann, L. Cobalt(III)-Catalyzed Hydroarylation of Allenes via C–H Activation. *ACS Catal.* **2017**, *7*, 2511-2515. (l) Mandal, R.; Sundararaju, B. Cp*Co(III)-Catalyzed Annulation of Carboxylic Acids with Alkynes. *Org. Lett.* **2017**, *19*, 2544-2547. (m) Zhou, X.; Luo, Y.; Kong, L.; Xu, Y.; Zheng, G.; Lan, Y.; Li, X. Cp*Co(III)-Catalyzed Branch-Selective Hydroarylation of Alkynes via C–H Activation: Efficient Access to α-Gem -Vinylindoles. *ACS Catal.* **2017**, *7*, 7296–7304. (n) Kuppusamy, R.; Santhoshkumar, R.; Boobalan, R.; Wu, H. R.; Cheng, C. H. Synthesis of 1,2-Dihydroquinolines by Co(III)-Catalyzed [3 + 3] Annulation of Anilides with Benzylallenes. *ACS Catal.* **2018**, *8*, 1880-1883. (o) Shankar, M.; Saha, A.; Sau, S.; Ghosh, A.; Gandon, V.; Sahoo, A. K. Harnessing Sulfur and Nitrogen in the Cobalt(III)-Catalyzed Unsymmetrical Double Annulation of Thioamides: Probing the Origin of Chemo- And Regio-Selectivity. *Chem. Sci.* **2021**, *12*, 6393-6405. (p) Ramachandran, K.; Anbarasan, P. Cobalt-Catalyzed Multisubstituted Allylation of the Chelation-Assisted C–H Bond of (Hetero)Arenes with Cyclopropenes. *Chem. Sci.* **2021**, *12*, 13442–13449.

10. (a) March, J. Advanced Organic Chemistry: Reactions, Mechanism, and Structures, 4th ed.; John Wiley & Sons, 1992; p 536. (b) Holleman, A. F.; Hartogs, J. C.; Van der Linden, T. Quantitative Untersuchungen uber Die Nitrierung Des Anilins. *Ber. Dtsch. Chem. Ges.* **1911**, *44*, 704–728. (c) Shen, H.; Vollhardt, K. P. C. Remarkable Switch in the Regiochemistry of the Iodination of Anilines by *N*-Iodosuccinimide: Synthesis of 1,2-Dichloro-3,4-Diiodobenzene. *Synlett* **2012**, *23*, 208–214. For a reaction through *para*-blocking strategy, see: (d) Midya, S. P.; Sahoo, M. K.; Landge, V. G.; Rajamohanan, P. R.; Balaraman, E. Reversed Reactivity of Anilines with Alkynes in the Rhodium-Catalysed C–H Activation/Carbonylation Tandem. *Nat. Commun.* **2015**, *6*, 8591. For reactions enabled by electrostatic-interaction, see: (e) Smith, M. R.; Bisht, R.; Haldar, C.; Pandey, G.; Dannatt, J. E.; Ghaffari, B.; Maleczka, R. E.; Chattopadhyay, B. Achieving High Ortho Selectivity in Aniline C–H Borylations by Modifying Boron Substituents. *ACS Catal.* **2018**, *8*, 6216-6223. (f) Naksomboon, K.; Poater, J.; Bickel-

haupt, F. M.; Fernández-Ibáñez, M. Á. Para-Selective C–H Olefination of Aniline Derivatives via Pd/S, O-Ligand Catalysis. *J. Am. Chem. Soc.* **2019**, *141*, 6719-6725. Also for *N*-substituted aniline derivatives, see: (g) Crampton, M. R.; Rabbitt, L. C.; Terrier, F. Electrophilic Aromatic Substitution in Substituted Anilines; Kinetics of the Reaction with 4,6-Dinitrobenzofuroxan. *Can. J. Chem.* **1999**, *77*, 639–646. (h) Kobayashi, S.; Komoto, I.; Matsuo, J. I. Catalytic Friedel-Crafts Acylation of Aniline Derivatives. *Adv. Synth. Catal.* **2001**, *343*, 71–74. (i) Ciana, C. L.; Phipps, R. J.; Brandt, J. R.; Meyer, F. M.; Gaunt, M. J. A Highly Para-Selective Copper(II)-Catalyzed Direct Arylation of Aniline and Phenol Derivatives. *Angew. Chem., Int. Ed.* **2011**, *50*, 458–462.

11. For selected reactions with vinyl cyclopropanes, see: (a) Wu, J. Q.; Qiu, Z. P.; Zhang, S. S.; Liu, J. G.; Lao, Y. X.; Gu, L. Q.; Huang, Z. S.; Li, J.; Wang, H. Rhodium(III)-Catalyzed C–H/C–C Activation Sequence: Vinylcyclopropanes as Versatile Synthons in Direct C–H Allylation Reactions. *Chem. Commun.* **2015**, *51*, 77-80. (b) Zell, D.; Bu, Q.; Feldt, M.; Ackermann, L. Mild C–H/C–C Activation by Z -Selective Cobalt Catalysis. *Angew. Chem., Int. Ed.* **2016**, *55*, 7408-7412. (c) Hu, Z.; Hu, X. Q.; Zhang, G.; Gooßen, L. J. Ring-Opening Ortho-C–H Allylation of Benzoic Acids with Vinylcyclopropanes: Merging Catalytic C–H and C–C Activation Concepts. *Org. Lett.* **2019**, *21*, 6770-6773. (d) Tanaka, R.; Tanimoto, I.; Kojima, M.; Yoshino, T.; Matsunaga, S. Imidate as the Intact Directing Group for the Cobalt-Catalyzed C–H Allylation. *J. Org. Chem.* **2019**, *84*, 13203-13210. (e) Wang, Q.; Zhi, C. L.; Lu, P. P.; Liu, S.; Zhu, X.; Hao, X. Q.; Song, M. P. Rhodium(III)-Catalyzed Direct C-7 Allylation of Indolines via Sequential C–H and C–C Activation. *Adv. Synth. Catal.* **2019**, *361*, 1253-1258. (f) Chen, H. M.; Liao, G.; Xu, C. K.; Yao, Q. J.; Zhang, S.; Shi, B. F. Merging C–H and C–C Activation in Pd(II)-Catalyzed Enantioselective Synthesis of Axially Chiral Biaryls. *CCS Chem.* **2021**, *3*, 455–465. (g) Keshri, S. K.; Madhavan, S.; Kapur, M. Catalyst-Controlled Chemodivergent Reactivity of Vinyl Cyclopropanes: A Selective Approach toward Indoles and Aniline Derivatives. *Org. Lett.* **2022**, *24*, 9043-9048. (h) Mandal, S.; Karjee, P.; Saha, S.; Punniyamurthy, T. Directed C8-H Allylation of Quinoline N -Oxides with Vinylcyclopropanes via Sequential C–H/C–C Activation. *Chem. Commun.* **2023**, *59* , 2823–2826.

12. (a) Gunanathan, C.; Milstein, D. Applications of Acceptorless Dehydrogenation and Related Transformations in Chemical Synthesis. *Science* **2013**, *341*, 1761–1779. (b) Vellakkaran, M.; Singh, K.; Banerjee, D. An efficient and selective Nickel-Catayzed Direct *N*-Alkylation of Amines with Alcohols. *ACS Catal.* **2017**, *7*, 8152-8158.

13. (a) Ma, W.; Mei, R.; Tenti, G.; Ackermann, L. Ruthenium(II)-Catalyzed Oxidative C–H Alkenylations of Sulfonic Acids, Sulfonyl Chlorides and Sulfonamides. *Chem. Eur. J.* **2014**, *20*, 15248–15251. (b) Wang, Y.; Du, C.; Wang, Y.; Guo, X.; Fang, L.; Song, M. P.; Niu, J. L.; Wei, D. High-Valent Cobalt-Catalyzed C–H Activation/Annulation of 2-Benzamidopyridine 1-Oxide with Terminal Alkyne: A Combined Theoretical and Experimental Study. *Adv. Synth. Catal.* **2018**, *360*, 2668–2677. (c) Tan, E.; Quinonero, O.; Elena De Orbe, M.; Echavarren, A. M. Broad-Scope Rh-Catalyzed Inverse-Sonogashira Reaction Directed by Weakly Coordinating Groups. *ACS Catal.* **2018**, *8*, 2166–2172. (d) Wang, L.; Carrow, B. P. Oligothiophene Synthesis by a General C–H Activation Mechanism: Electrophilic Concerted Metalation-Deprotonation (ECMD). *ACS Catal.* **2019**, *9*, 6821–6836. (e) Rogge, T.; Oliveira, J. C. A.; Kuniyil, R.; Hu, L.; Ackermann, L. Reactivity-Controlling Factors in Carboxylate-Assisted C–H Activation under 4d and 3d Transition Metal Catalysis. *ACS Catal.* **2020**, *10*, 10551-10558.

14. Cobalt(III) species can adopt three spin states namely singlet, triplet, and quintet. However, some previous reports suggest that 18 electron cobalt complexes are most stable in the singlet state. We computed the energy for the rate-determining TS_{D-E} corresponding to the triplet spin state and found it to be 1.6 kcal/mol higher than the singlet state. Consequently, we have not computed the energy of the triplet and quintet spin states in our DFT calculations as most of our intermediates are 18 electron complexes, and it is unlikely to change the analysis of our results. For related discussions, see: (a) Gandon, V.; Agenet, N.; Vollhardt, K. P. C.; Malacria, M.; Aubert, C. Cobalt-Mediated Cyclic and Linear 2:1 Cooligomerization of Alkynes with Alkenes: A DFT Study. *J. Am. Chem. Soc.* **2006**, *128*, 8509–8520. (b) Agenet, N.; Gandon, V.; Vollhardt, K. P. C.; Malacria, M.; Aubert, C. Cobalt-Catalyzed Cyclotrimerization of Alkynes: The Answer to the Puzzle of Parallel Reaction Pathways. *J. Am. Chem. Soc.* **2007**, *129*, 8860–8871.